Predicting Solid–Liquid Equilibrium of Fatty Acid Methyl Ester and Monoglyceride Mixtures as Biodiesel Model Fuels

AUTHOR(S):

Yoshidomi, Shinichiro; Sugami, Yuitsu; Minami, Eiji; Shisa, Noriko; Hayashi, Hitoshi; Saka, Shiro

Authors: Shinichiro Yoshidomi[1] · Yuitsu Sugami[1] · Eiji Minami[1] · Noriko Shisa[2] · Hitoshi Hayashi[2] · Shiro Saka[1]

Title: Predicting solid–liquid equilibrium of fatty acid methyl ester and monoglyceride mixtures as biodiesel model fuels

Affiliations and addresses:

[1] Graduate School of Energy Science, Kyoto University, Yoshida-honmachi, Sakyo-ku, Kyoto 606-8501, Japan

[2] Material Engineering Division, Toyota Motor Corporation, Toyota-cho, Toyota, Aichi 471-8572, Japan

Corresponding author: Shiro Saka

E-mail: saka@energy.kyoto-u.ac.jp. Tel/Fax: +81-75-753-4738.

Abstract Fatty acid methyl esters from plant oils are the main component of biodiesel and used as a substitute for petroleum diesel. Biodiesel generally contains a small amount of monoglycerides as intermediate compounds, which have high melting points and often solidify and clog fuel filters. The prediction of the cold-flow property of biodiesel is of great importance for practical application. In this study, a thermodynamic study was conducted for mixtures of monoglycerides and fatty acid methyl esters. Temperatures of the solid–liquid equilibrium for the mixtures were measured by differential scanning calorimetry and visual observation, while the theoretical values were calculated using the modified Universal Quasi-chemical Functional-group Activity Coefficients (UNIFAC) model (Dortmund). The theoretical and experimental results were in good agreement, especially for binary mixtures of monoglycerides and methyl esters. The importance of monoglycerides on the cold-flow properties of biodiesel was determined, and the effects could be well described by the modified UNIFAC model (Dortmund).

Keywords Biodiesel · Solid-liquid equilibrium · Fatty acid methyl ester · Monoglyceride

Introduction

Fatty acid methyl esters (FAMEs) produced from plant oils are the main constituent of biodiesel, which is widely used as an alternative to petroleum diesel. FAMEs are generally produced by transesterification of triglycerides, which are the main component of plant oils. Although biodiesel is attractive because it is a renewable energy source, it has some drawbacks owing to the differences in chemical structure from petroleum-derived diesel. Unsaturated double bonds in FAMEs are prone to oxidation, leading to poor stability in oxidizing conditions [1]. Moreover, saturated FAMEs such as methyl palmitate and methyl stearate have relatively high melting points and often solidify at low temperatures.

The use of biodiesel blended with petroleum diesel has being promoted in recent years, especially in Southeast Asian countries [2]. Indonesia started to use 20% biodiesel blended with petroleum diesel (B20) in 2016. The Indonesian government also plans to implement a B30 policy in 2020 [3]. However, there is a concern that the above-mentioned drawbacks may become problematic when the blend ratio of biodiesel increases. Dunn and Bagby have reported that a high concentration of biodiesel in blends causes deterioration of the cold-flow property of the fuel [4]. This leads to clogging of fuel filters, and thus engine stalling may occur. Predicting the cold-flow property of a biodiesel blend is of great importance to minimize the risk of fuel clogging.

Cloud point (CP) is an indicator of the cold-flow property of a fluid, defined in ISO 3015 [5] as the temperature at which a cloud of wax crystals first appears in a liquid when it is cooled under specified conditions. Simple linear regression analyses have been undertaken for the CP prediction of biodiesels and the models obtained had relatively good correlation with experimental results [6–8]. However, these models are not applicable to all biodiesels because they were established using only a few feedstocks. Our research group has predicted CPs based on the solid–liquid equilibrium of FAME mixtures, as established in a previous

study [9]. The theoretical and experimental values were consistently in a good agreement each other, even with the assumption of simple ideal solution. This finding has been supported by some other groups [10, 11], and this thermodynamic approach has proven to work well for CP prediction.

These predictions were only used for high-purity biodiesel composed of only FAMEs. A small amount of monoglycerides (MGs) and diglycerides (DGs) are included as intermediate compounds as well as unreacted triglycerides in real biodiesel. MG has a higher melting point than the corresponding methyl ester and solidifies easily at low temperatures. Tang et al. have reported that the insoluble precipitate from palm oil-based biodiesel consisted mainly of MGs [12] and Chupka et al. found that the amount of saturated MGs highly affected the CP of biodiesel blend [13]. MGs have several polymorphic crystalline forms referred to as α, β′ and β, and each has different melting point ($\alpha < \beta' < \beta$) [14]. The potential for several MG polymorphs makes the cold-flow property of biodiesel complicated. Chupka et al. have applied the ideal solution model for the calculation of solid–liquid equilibrium to predict the CP of biodiesel containing MGs but found a large deviation between the experimental and predicted values [15]. This implies that a mixture of MGs and FAMEs behaves as a non-ideal solution unlike a mixture of only FAMEs.

As mentioned above, calculating the solid–liquid equilibrium of biodiesel would become a powerful method to predict the cold-flow property. Since real biodiesel is a complex mixture of FAMEs, MGs, antioxidant and so on, we need to determine thermodynamic interactions between these components to calculate the equilibrium exactly. Precipitation may be caused by MGs or saturated FAMEs. The effect of saturated FAMEs have already been elucidated in the previous paper [9], therefore, this study attempts to elucidate the thermodynamic interactions between MGs and FAMEs using their binary and multi-component mixtures, taking non-ideality of liquid phase into consideration. Although

this study was conducted with biodiesel model fuels, the knowledge obtained would be valuable to establish a sophisticated prediction method for real biodiesel.

Materials and Methods

Materials

In typical plant oils, palmitic (C16:0), stearic (C18:0), oleic (C18:1), linoleic (C18:2) and linolenic (C18:3) acids are the major fatty acids. Palmitic acid is the main saturated fatty acids especially in palm oil, while oleic acid is a representative of unsaturated ones in almost plant oils including palm oil. The MGs of palmitic acid are probably an important cause of precipitation because they are saturated MGs and have higher melting points than unsaturated MGs. Hence, we chose a binary mixture of 1-monopalmitin and methyl oleate as a model for biodiesel from typical plant oils. Coconut and palm kernel oils are different from most plant oils because they are composed of shorter fatty acids including lauric acid (C12:0). A binary mixture of 1-monolaurin and methyl laurate was also studied as a model for fuel from coconut and palm kernel oils. However, the choice of the components in binary mixtures is not a significant concern in this study, because our primary purpose is to discuss the effect of non-ideality in MG and FAME mixtures on the calculation of solid–liquid equilibrium. Finally, some multi-component mixtures of MGs and FAMEs were also evaluated.

1-Monolaurin (C12:0 MG, >98%) and 1-monopalmitin (C16:0 MG, 98%) were purchased from Tokyo Chemical Industry Co., Ltd., Tokyo, Japan, while 1-monoolein (C18:1 MG, >99%), methyl laurate (C12:0 FAME, 99.5%), methyl palmitate (C16:0 FAME, >99%), methyl oleate (C18:1 FAME, >99%), and methyl linoleate (C18:2 FAME, >99%) were obtained from Sigma-Aldrich Japan Co., LLC., Tokyo, Japan. All chemicals were used without purification.

Experimental Methods and Definitions

Differential scanning calorimetry (DSC) was performed using a DSC-50 system (Shimadzu Corp.) to evaluate the solid–liquid equilibrium of samples in non-hermetic aluminum-based pans under dry nitrogen flow. Indium and zinc were used for the temperature calibration and α-alumina was used as a reference material. Heating and cooling rates were set to 10 and -3 °C/min, respectively. Each sample was heated until fully melted for each measurement and then cooled until the first phase transition was observed from liquid to solid. The sample was then reheated until the solid phase melted and the temperature of the endothermic peak top was defined as the solid–liquid equilibrium temperature (T_{SLE}) [16]. The reason that the T_{SLE} was measured on the heating cycle was to remove the effect of supercooling. Therefore, the measured T_{SLE} will be slightly higher than the CP, because CP occurs during the cooling cycle and often includes a supercooling effect. The melting point and enthalpy of fusion were also estimated for each pure component based on the onset temperature of the endothermic peak from the DSC heating curve [16], and the values obtained were used to calculate the solid–liquid equilibrium.

Visual observation was conducted using a glass cell apparatus developed by Matsuda et al. [17] (Fig. 1) when the concentration of MG was less than 2 wt% because the endothermic peak was too small to detect at such low concentrations on DSC. Approximately 10 mL of the melted sample was placed in the sample cell (inner diameter, 20 mm; height, 150 mm) for each observation and cooled with agitation until solid substance formed. The temperature at which solids formed was defined as the solidification temperature on cooling (T_S). The sample was then heated maintaining agitation, and the temperature at which the solid substance completely melted was defined as the melting temperature on heating (T_M). The heating and cooling rates were approximately 1 and -1 °C/min, respectively.

Thermodynamic Model

The solid–liquid equilibrium can be thermodynamically expressed as the equality of fugacities in solid and liquid phases (f_i^{L*} and f_i^{S*}, respectively) for each component *i* by the following equation:

$$f_i^{L*} = f_i^{S*}, thus\ \gamma_i^L x_i f_i^L = \gamma_i^S z_i f_i^S \qquad (1)$$

where γ_i^L and γ_i^S are activity coefficients of component *i*, and f_i^L and f_i^S are fugacities of pure component *i* in liquid and solid phases, respectively. The x_i and z_i terms are mole fractions of component *i* in liquid and solid phases, respectively. Furthermore, the fugacity ratio of a pure component in solid and liquid phases can be described as follows [18]:

$$\frac{f_i^L}{f_i^S} = \exp\left[\left(\frac{T_{SLE} - T_{m,i}}{RT_{SLE}}\right)\left(\frac{\Delta H_{m,i}}{T_{m,i}}\right)\right] = \frac{\gamma_i^L x_i}{\gamma_i^S z_i} \qquad (2)$$

where $\Delta H_{m,i}$ and $T_{m,i}$ are enthalpy of fusion and the melting point of each component *i*, respectively. It should be noted that the term of heat capacity is already omitted in this equation because it is usually small enough to be non-consequential [18].

We assumed that the solid phase that formed at T_{SLE} is composed of only a single-component and both z_i and γ_i^S are equal to unity. This assumption is not always true but in the case of a binary mixture of MG and FAME it is probably a plausible approximation because their chemical structures are clearly different and may not form a mixed crystal.

The Universal Quasi-chemical Functional-group Activity Coefficients (UNIFAC) model is well-established tool that can incorporate intra- and intermolecular contributions based on the functional groups of each molecule in a mixture to estimate the activity coefficient (γ_i^L) [19]. We used a modified UNIFAC model developed by Gmehling et al., referred hereinafter to as “UNIFAC (Dortmund)”, to calculate γ_i^L because it can be applied to wide range of temperature [20]. The calculation was conducted using a program coded with Microsoft Visual Basic for Applications 7.0 in Excel 2010.

Results and Discussion

Properties of Pure Component

Table 1 shows the melting point and enthalpy of each pure component measured by DSC, along with the numbers of functional groups of each compound. The properties of the MGs were estimated considering their polymorphic behavior. Generally α type crystals form first when a pure MG is cooled until the phase transition occurs from liquid to solid. The α crystals convert irreversibly to the β′ structure and then to the most stable β form after a certain transition time [21]. The transition times tend to be faster for MGs with shorter chains and more degrees of unsaturation [22]. High temperature and presence of the solvent also shorten the transition times [22]. For these reasons, the melting point and enthalpy of α type MGs were measured by heating the sample immediately after the solid phase had formed. The properties of the β′ and β type crystals were measured after a certain transition time has passed. The transition times were extremely fast for 1-monolaurin and 1-monoolein and the α type structures quickly converted into the β form. Therefore, it was difficult to measure the enthalpy of fusion for the β′ type of these compounds.

There are many publications reporting the thermodynamic properties of various FAMEs and MGs, such as melting point and enthalpy [23–26]. The values measured in this study were consistent with those previously reported, and the values obtained were applied for the calculation of solid–liquid equilibriums. However, the enthalpies of β′ type monolaurin and monoolein have not been reported, probably because of the difficulty of measuring this transition.

Binary Mixture

Figure 2 shows the DSC curves for the binary mixture of 30 wt% 1-monopalmitin and 70 wt% methyl oleate. An exothermic peak was observed at 46.6 °C on cooling the liquid sample (a), which is related to the formation of α type monopalmitin. Immediately exposing the sample to heating after the α type crystals formed resulted in an endothermic peak at 51.5 °C (b), which can be assigned to the T_{SLE} of the α type monopalmitin. When the sample was heated 6 hours (c) or 11 days (d) after the α type crystals formed the endothermic peaks shift to higher temperatures at 59.5 °C and 66.4 °C, respectively, which are the T_{SLE} values of the β′ and β type crystals, respectively.

The binary mixture of 1-monopalmitin and methyl oleate was studied in the same way at various concentrations and each T_{SLE} of the crystalline types are shown in Fig. 3. As already reported by Chupka et al. [15], the ideal solution model ($\gamma_i^L = 1$) (shown as a dashed line) has a large deviation from the experimental results (shown as filled circles) for every crystalline form. However, the UNIFAC (Dortmund) model (shown as a solid line) provides excellent agreement with the experimental values. Similar analyses for a binary mixture of 1-monolaurin and methyl laurate are shown in Fig. 4. Although there is a small deviation for the α type structure, it is obvious that the UNIFAC (Dortmund) model fits well with the experimental results. The T_{SLE} of β′ monolaurin was not measureable because of the fast transition from β′ to β crystalline form.

These results show that the modified UNIFAC (Dortmund) model accounts for the non-ideality in MG and FAME mixtures, and the solid–liquid equilibrium is well predicted for the different types of FAMEs, MGs and their crystalline structures. The γ_i^L at the eutectic point for various binary mixtures were calculated to discuss the degree of non-ideality (Table 2). Activity coefficients were estimated to be almost unity by the UNIFAC (Dortmund) model for binary mixtures of only FAMEs. This is why CPs were successfully predicted for mixtures of only FAMEs in the previous study [9], even assuming an ideal solution ($\gamma_i^L = 1$).

MG in FAME has a large activity coefficient; for example, γ_i^L=59 for 1-monolaurin in methyl linoleate. This means that MG in FAME shows remarkable non-ideality, and solids form easily, even if the concentration is quite low.

Visual observation was conducted for the sample containing less than 2 wt% of MG (Fig. 5). For monopalmitin in methyl oleate (a), the sample was cooled with agitation and the solidification temperature (T_S) was measured (indicated by open circles). The sample was then heated and the melting temperature (T_M) of the solid phase was also estimated (filled circles). The measured T_S and T_M correspond completely with the T_{SLE} values calculated by the UNIFAC (Dortmund) model for the β′ and β type structures, respectively. Similar behaviors were observed for monolaurin in methyl laurate (b). It should be noted that the T_{SLE} values of β′ monolaurin (dashed line) was calculated assuming a tentative value of 27,000 J/mol as the enthalpy of fusion because it was not measurable by DSC.

The reason MG solidifies at the T_{SLE} of β′ during the visual observation can probably be explained as follows: the MG is not supercooled under agitation with a slow cooling rate, so solidification occurs immediately when the temperature reaches the T_{SLE} of β′. Once the solid phase formed, it did not melt until the temperature exceeded the T_{SLE} of β, even if the sample was immediately exposed to a heating cycle. It appears that the β′ structure of MG was quickly converted into β under the given conditions. Although the reason for these behaviors remain unclear, it is possible that the β′ form is partly dissolved in FAME on the heating cycle but immediately solidified as the β form, and this process is repeated until the transition is finished. This mechanism is generally known as Ostwald's rule of stages for the transition of polymorphs in a solvent [27]. However, further study is needed to explore the behaviors of MG in FAME.

Multi-Component Mixture

Our study was extended to multi-component mixtures prepared by blending various MGs and FAMEs. The T_S and T_M were measured by visual observation (Table 3). The measured T_S and T_M values are close to the calculated T_{SLE} values of the β′ and β structures of the MGs, respectively. Hence, similar phenomena seem to occur in these multi-component mixtures as those in the binary mixtures (Fig. 5). Samples 1 to 5 — which contain two kinds of MGs — had slight deviations between the measured and calculated values, whereas samples 6 and 7 — which contain only one MG — were almost consistent with the calculated values.

The solid phase was assumed to be formed as a single component (i.e., $z_i\gamma_i^S = 1$) for the calculation of the solid–liquid equilibrium. This assumption is probably appropriate when the mixture contains only one MG. However, in cases including two or more MGs, the MGs could cocrystallize (i.e., $z_i\gamma_i^S \neq 1$). Maruyama et al. have reported a mixed crystal (solid solution) composed of different MGs [28]. Further studies on the effect of solid solutions of MGs are needed to allow precise prediction of the solid–liquid equilibrium of complex mixtures.

Conclusions

A series of model mixtures of MGs and FAMEs were studied to aid the prediction of cold-flow properties of biodiesel. Although remarkable non-ideality was found between MG and FAME, it was determined that the modified UNIFAC (Dortmund) model can successfully predict the non-ideality. Binary mixture of MG and FAME showed good agreement between the theoretical values and measured equilibrium temperatures. Our study was further extended to multi-component mixtures, and the theoretical and experimental values were also consistent. However, mixtures with two kinds of MGs deviated from the model to some extent, which might be caused by the effect of solid solution MGs. We need

further studies about the effect of cocrystallization of MGs to establish a practical prediction model for real biodiesel.

Conflict of Interest the authors declare that they have no conflicts of interest.

References

1. Moser BR (2009) Biodiesel production, properties, and feedstocks. Vitr Cell Dev Biol - Plant 45:229–266
2. Chanthawong A, Dhakal S (2016) Liquid biofuels development in southeast asian countries: an analysis of market, policies and challenges. Waste Biomass Valoriz 7:157–173
3. Kharina A, Malins C, Searle S (2016) Biofuels policy in Indonesia : overview and status report. White Paper of the International Counsil on Clean Transportation 1–17
4. Dunn RO, Bagby MO (1995) Low-temperature properties of triglyceride-based diesel fuels: transesterified methyl esters and petroleum middle distillate/ester blends. J Am Oil Chem Soc 72:895–904
5. International Organization for Standarization (ISO) (1992) Petroleum products: Determination of cloud point. ISO 3015:1992. 1–4
6. Sarin A, Arora R, Singh NP, Sarin R, Malhotra RK, Kundu K (2009) Effect of blends of Palm-Jatropha-Pongamia biodiesels on cloud point and pour point. Energy 34:2016–2021
7. Su YC, Liu YA, Diaz Tovar CA, Gani R (2011) Selection of prediction methods for thermophysical properties for process modeling and product design of biodiesel manufacturing. Ind Eng Chem Res 50:6809–6836
8. Dunn RO, Moser BR (2010) Cold weather properties and performance of biodiesel. In: Knothe G, Krahl J, Gerpen J Van (eds) The biodiesel handbook. 2nd ed. AOCS Press, Illinois, pp 147–204
9. Imahara H, Minami E, Saka S (2006) Thermodynamic study on cloud point of biodiesel with its fatty acid composition. Fuel 85:1666–1670

10. Lopes JCA, Boros L, Krähenbuühl MA, Meirelles AJA, Daridon JL, Pauly J, Marrucho IM, Coutinho JAP (2008) Prediction of cloud points of biodiesel. Energy Fuels 22:747–752
11. Coutinho JAP, Goncalves M, Pratas MJ, Batista MLS, Fernandes VFS, Pauly J, Daridon JL, Gonçalves M, Pratas MJ, Batista MLS, Fernandes VFS, Pauly J, Daridon JL (2010) Measurement and modeling of biodiesel cold-flow properties. Energy Fuels 24:2667–2674
12. Tang H, De Guzman RC, Salley SO, Ng KYS (2008) Formation of insolubles in palm oil-, yellow grease-, and soybean oil-based biodiesel blends after cold soaking at 4 °C. J Am Oil Chem Soc 85:1173–1182
13. Chupka GM, Fouts L, Lennon JA, Alleman TL, Daniels DA, Mccormick RL (2014) Saturated monoglyceride effects on low-temperature performance of biodiesel blends. Fuel Process Technol 118:302–309
14. Lutton ES, Jackson FL (1948) The polymorphism of 1-monostearin and 1-monopalmitin. J Am Oil Chem Soc 70:2245–2249
15. Chupka GM, Yanowitz J, Chiu G, Alleman TL, Mccormick RL (2011) Effect of saturated monoglyceride polymorphism on low-temperature performance of biodiesel. Energy Fuels 25:398–405
16. Matsuoka M, Ozawa R (1989) Determination of solid-liquid phase equilibria of binary organic systems by differential scanning calorimetry. J Cryst Growth 96:596–604
17. Matsuda H, Kimura H, Nagano Y, Kurihara K, Tochigi K, Ochi K (2011) Solid-liquid equilibria in three binary mixtures containing diphenyl carbonate. J Chem Eng Data 56:1500–1505
18. Smith J.M., Van Ness HC, Abbott MM (2005) Introduction to chemical engineering thermodynamics, 7th ed. McGraw-Hill, New York

19. Fredenslund A, Jones RL, Prausnitz JM (1975) Group-contribution estimation of activity coefficients in nonideal liquid mixtures. AIChE J 21:1086–1099

20. Gmehling J, Li J, Schiller M (1993) A modified UNIFAC model. 2. Present parameter matrix and results for different thermodynamic properties. Ind Eng Chem Res 32:178–193

21. Maruyama T, Niiya I, Imamura M, Okada M, Matsumoto T (1973) Study on polymorphism of monoglyceride . II. Thermodynamic considerations on transition. J Japan Oil Chem Soc 22:85–88(in Japanese)

22. Maruyama T, Isao N, Imamura M, Okada M, Matsumoto T, Horisawa M, Matsumoto T (1971) Study on polymorphism of monoglyceride. I. Transition of crystal modification of 1-monolaurin, 1-monomyristin, 1-monopalmitin and 1-monostearin. J Japan Oil Chem Soc 20:395–402(in Japanese)

23. Lutton ES (1971) The phases of saturated 1-monoglycerides C14-C22. J Am Oil Chem Soc 48:778–781

24. Knothe G, Dunn RO (2009) A comprehensive evaluation of the melting points of fatty Acids and esters determined by differential scanning calorimetry. J Am Oil Chem Soc 86:843–856

25. Dunn RO (2008) Crystallization behavior of fatty acid methyl esters. J Am Oil Chem Soc 85:961–972

26. Maruyama T, Niiya I, Okada M, Matsumoto T (1979) Studies on polymorphism of monoglycerides. X. Transition of crystal modification of cis-monounsaturated monoglycerides. J Japan Oil Chem Soc 28:486–490(in Japanese)

27. Ostwald W (1897) Studies on formation and transformation of solid materials. Z Phys Chem 22:289–330

28. Maruyama T, Niiya I, Okada M, Matsumoto T (1979) Studies on polymorphism of monoglycerides. VIII. Phase behaviour of binary monoglycerides systems. J Japan Oil Chem Soc 28:100–105(in Japanese)

List of Tables

List of Figures

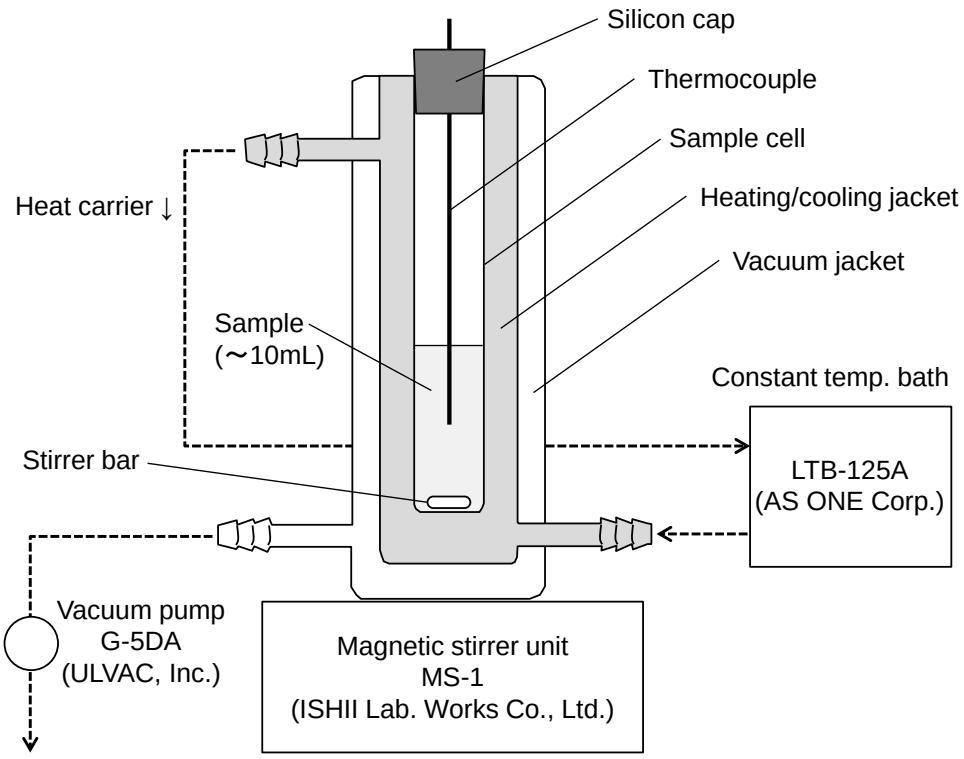

Fig. 1

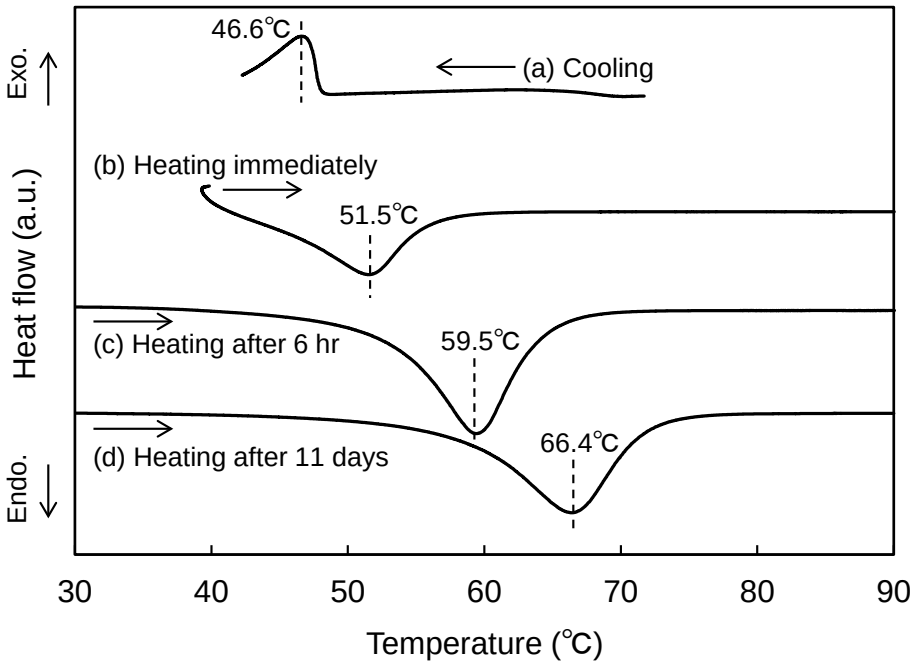

Fig. 2

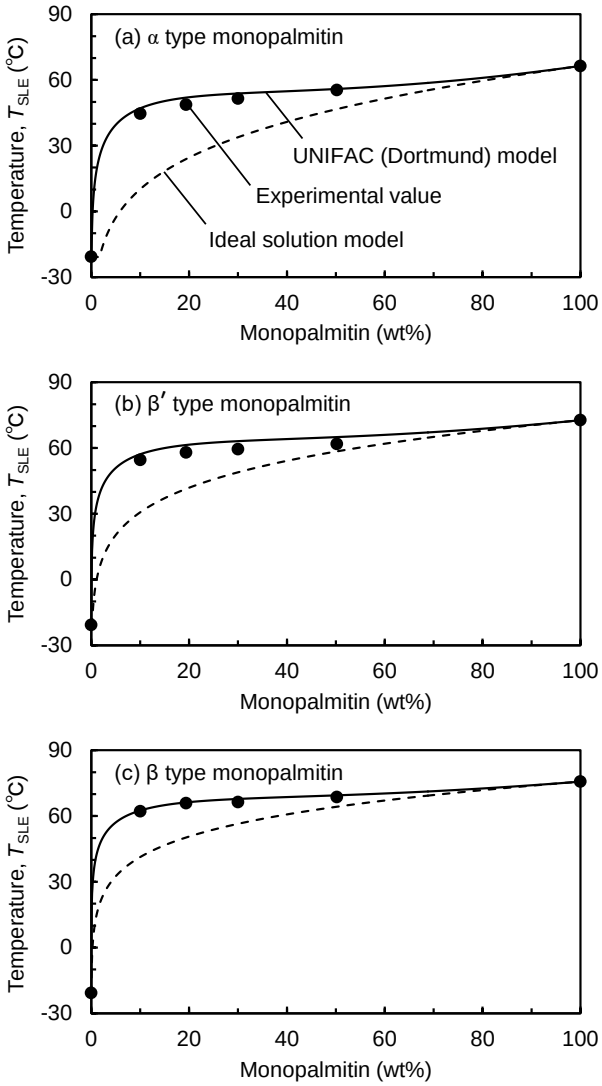

Fig. 3

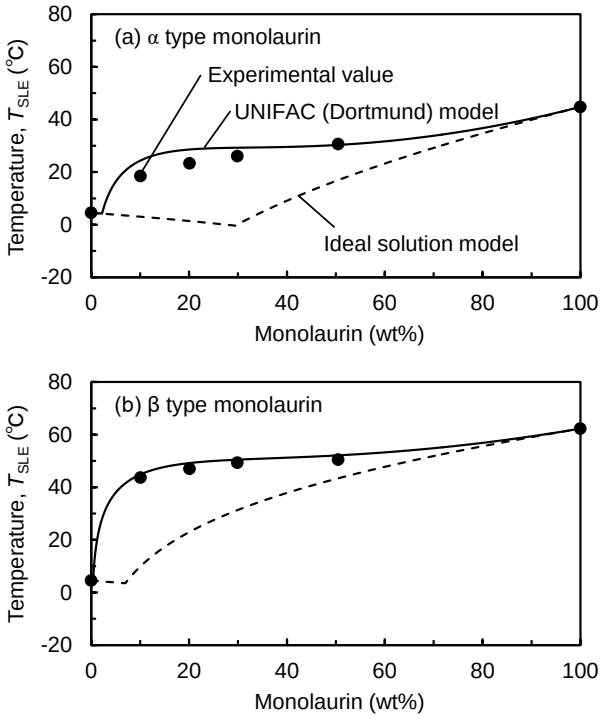

Fig. 4

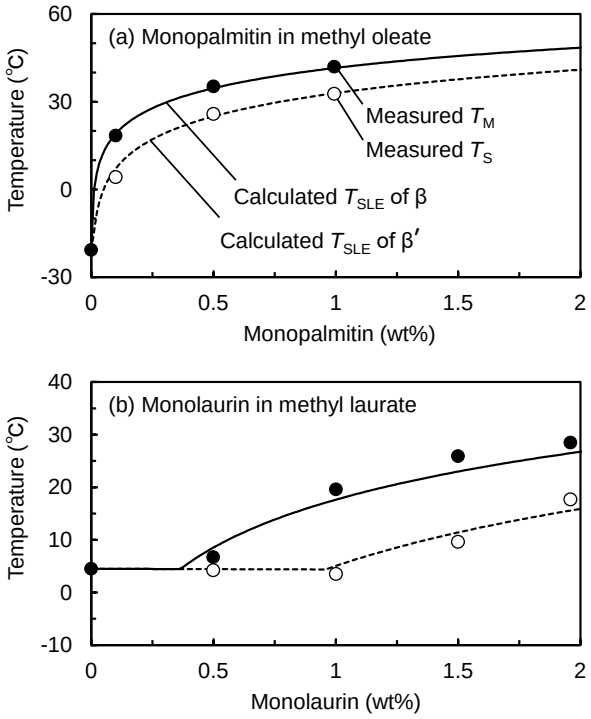

Fig. 5

Table 1 Properties of each pure component used to calculate solid–liquid equilibria

Component	Type	Melting point (°C)	Enthalpy of fusion (J/mol)	Number of functional groups						
				CH_3	CH_2	CH	CH=CH	OH(p)	OH(s)	CH_2COO
FAME										
Methyl laurate (C12:0)		4.5	36,400	2	9	0	0	0	0	1
Methyl palmitate (C16:0)		29.8	60,400	2	13	0	0	0	0	1
Methyl oleate (C18:1)		-20.7	41,600	2	13	0	1	0	0	1
Methyl linoleate (C18:2)		-42.4	36,200	2	11	0	2	0	0	1
MG										
1-monolaurin (C12:0)	α	44.8	22,400	1	11	1	0	1	1	1
	β′	59.5	-							
	β	62.3	38,000							
1-monopalmitin (C16:0)	α	66.4	34,100	1	15	1	0	1	1	1
	β′	72.7	49,900							
	β	75.7	63,600							
1-monoolein (C18:1)	α	15.0*	11,000*	1	15	1	1	1	1	1
	β′	30.1	-							
	β	35.0	49,400							

* From reference [26]

- Not measureable because of fast transition

Table 2 Activity coefficients γ_i^L calculated by the modified UNIFAC (Dortmund) model in binary mixtures of FAME and MG at the eutectic point

Solute	Solvent	Eutectic point		γ_i^L of solute
		Fraction (wt% of solute)	Temperature (°C)	
Methyl palmitate	Methyl laurate	11.65	2.8	1.009
	Methyl oleate	0.75	-20.7	1.001
	Methyl linoleate	0.06	-41.7	1.008
1-monolaurin (α)	Methyl laurate	2.22	4.3	16.679
	Methyl oleate	0.22	-20.7	46.870
	Methyl linoleate	0.07	-42.4	59.000
1-monopalmitin (α)	Methyl laurate	0.83	4.5	12.643
	Methyl oleate	0.06	-20.7	31.099
	Methyl linoleate	0.01	-42.4	39.235

Table 3 Chemical compositions of the multi-component mixtures and the measured T_S and T_M by visual observation compared with the calculated T_{SLE} for β′ and β structures of MG

Sample No.	Composition of the mixture (wt%)							Measured (°C)		Calculated T_{SLE} (°C)	
	Methyl esters				1-monoglycerides						
	Laurate (C12:0)	Palmitate (C16:0)	Oleate (C18:1)	Linoleate (C18:2)	Laurin (C12:0)	Palmitin (C16:0)	Olein (C18:1)	T_S	T_M	β′	β
1	49.52	-	49.48	-	0.50	0.50	-	15.6	26.0	19.4	30.2
2	-	9.45	19.93	70.09	-	0.10	0.43	5.3	16.0	5.1	17.3
3	-	13.95	75.04	9.96	-	0.21	0.84	9.8	22.2	13.8	25.0
4	-	40.64	49.43	8.90	-	0.50	0.53	16.6	32.2	23.8	33.7
5	65.17	23.95	9.88	-	0.71	0.29	-	11.0	20.6	12.1	23.7
6	49.49	-	49.51	-	-	1.00	-	28.3	37.0	28.4	37.7
7	-	13.96	75.52	10.31	-	0.21	-	15.0	25.4	14.9	25.9